A remote sensing model to estimate ecosystem respiration in Northern China and the Tibetan Plateau

Yanni Gao [a,b], Guirui Yu [a,*], Shenggong Li [a], Huimin Yan [a,*], Xianjin Zhu [a,c], Qiufeng Wang [a], Peili Shi [a], Liang Zhao [d], Yingnian Li [d], Fawei Zhang [d], Yanfen Wang [c], Junhui Zhang [e]

[a] Synthesis Research Center of Chinese Ecosystem Research Network, Key Laboratory of Ecosystem Network Observation and Modeling, Institute of Geographic Sciences and Natural Resources Research, Chinese Academy of Sciences, Beijing 100101, China
[b] State Key Laboratory of Environmental Criteria and Risk Assessment, Chinese Research Academy of Environmental Sciences, Beijing 100012, China
[c] University of Chinese Academy of Sciences, Beijing 100049, China
[d] Northwest Institute of Plateau Biology, Chinese Academy of Sciences, Xining 810001, China
[e] Institute of Applied Ecology, Chinese Academy of Sciences, Shenyang 110016, China

ABSTRACT

Ecosystem respiration (R_e) is rarely quantified from remote sensing data because satellite technique is incapable of observing the key processes associated with soil respiration. In this study, we develop a Remote Sensing Model for R_e (ReRSM) by assuming that one part of R_e is derived from current photosynthate with the respiratory rate coupling closely with gross primary production (GPP), and the other part of R_e is derived from reserved ecosystem organic matter (including plant biomass, plant residues and soil organic matter) with the respiratory rate responding strongly to temperature change. The ReRSM is solely driven by the Enhanced Vegetation Index (EVI), the Land Surface Water Index (LSWI) and the Land Surface Temperature (LST) from MODIS data. Multi-year eddy CO_2 flux data of five vegetation types in Northern China and the Tibetan Plateau (including temperate mixed forest, temperate steppe, alpine shrubland, alpine marsh and alpine meadow-steppe) were used for model parameterization and validation. In most cases, the simulated R_e agreed well with the observed R_e in terms of seasonal and interannual variation irrespective of vegetation types. The ReRSM could explain approximately 93% of the variation in the observed R_e across five vegetation types, with the root mean square error (RMSE) of 0.04 mol C m^{-2} d^{-1} and the modeling efficiency (EF) of 0.93. Model comparison showed that the performance of the ReRSM was comparable with that of the RECO in the studied five vegetation types, while the former had much fewer parameters than the latter. The ReRSM parameters showed good linear relationships with the mean annual satellite indices. With these linear functions, the ReRSM could explain approximately 90% of the variation in the observed R_e across five vegetation types, with the RMSE of 0.05 mol C m^{-2} d^{-1} and the EF of 0.89. These analyses indicated that the ReRSM is a simple and alternative approach in R_e estimation and has the potential of estimating spatial R_e. However, the performance of ReRSM in other vegetation types or regions still needs a further study.

© 2015 Elsevier B.V. All rights reserved.

1. Introduction

Net ecosystem CO_2 exchange (NEE) is one of the main drivers for interannual variation in atmosphere CO_2 concentration (Trumbore, 2006). NEE is a small difference between two large fluxes of gross primary production (GPP) and ecosystem respiration (R_e). Accurate estimation of the spatio-temporal variation in NEE depends on the robust estimates of GPP and R_e.

Remote sensing (RS) technology has been used as a major tool in quantifying carbon balance of ecosystems at regional and global scales because it monitors ecosystem structure at high temporal and spatial resolution (Running et al., 2004; Rahman et al., 2005). There are various satellite-driven GPP models for estimating spatial GPP distribution from remote sensing data (e.g., Xiao et al., 2004; Running et al., 2004; Gitelson et al., 2006, 2012; Yuan et al., 2007; Sims et al., 2008; Wu et al., 2010). Yet, we lack similar methods for R_e estimation.

Ecosystem respiration is composed of different components that are determined by different mechanisms and factors. It is

* Corresponding authors at: Institute of Geographic Sciences and Natural Resources Research, Chinese Academy of Sciences, 11A, Datun Road, Chaoyang District, Beijing 100101, China. Tel.: +86 10 64889432.

E-mail addresses: yugr@igsnrr.ac.cn (G. Yu), yanhm@igsnrr.ac.cn (H. Yan).

difficult for satellite technology to monitor various respiratory processes, especially those in the soil (Valentini et al., 2000; Running et al., 2004; Olofsson et al., 2008; Xiao et al., 2008; Tang et al., 2012), which limit the application of remote sensing data in R_e estimation. However, R_e showed close relationships with easily satellite-retrieved GPP (e.g., Knohl et al., 2005; Tang et al., 2005; Moyano et al., 2007, 2008; Larsen et al., 2007; Bahn et al., 2008; Gomez-Casanovas et al., 2012; Huang and Niu, 2013) and temperature (e.g., Lloyd and Taylor, 1994; Frank et al., 2002; Reichstein et al., 2003; Bond-Lamberty and Thomson, 2010) in most of ecosystems, and upon these relationships some empirical or semi-empirical satellite-driven R_e models were developed and validated at the plot or regional scale (Vourlitis et al., 2003; Gilmanov et al., 2005; Rahman et al., 2005; Schubert et al., 2010; Jägermeyr et al., 2014). However, extensive studies reported that the responses to GPP and temperature varied among the R_e components (e.g., Gaumont-Guay et al., 2008; Kuzyakov and Gavrichkova, 2010), and the current satellite-driven R_e models almost all neglected these differences. Therefore, we will develop a new Remote Sensing Model for R_e (ReRSM) based on the different responses of R_e components to the variations in GPP and temperature. Long-term eddy CO_2 flux data of five vegetation types (located in Northern China and the Tibetan Plateau) from the ChinaFLUX were used to assess the model performance. We also compared the estimated accuracy of the ReRSM with that of the RECO, which was a totally satellite-driven R_e model (Jägermeyr et al., 2014).

2. Materials and methods

2.1. Description of the ReRSM

Ecosystem respiration is mainly composed of five components (Fig. 1). They are plant growth respiration (R_g) and maintenance respiration (R_m) belonging to autotrophic respiration (R_a), and rhizomicrobial respiration (R_{rhi}, i.e., microbial respiration of rhizodeposits derived from living roots), microbial respiration of plant residues (R_{res}) and SOM decomposition (R_{SOM}) belonging to heterotrophic respiration (R_h).

$$R_e = R_g + R_m + R_{rhi} + R_{res} + R_{SOM} \qquad (1)$$

It was reported that the substrates for plant growth respiration (R_g) (Amthor, 2000; Piao et al., 2010; Mahecha et al., 2010; Chapin et al., 2011) and rhizomicrobial respiration (R_{rhi}) (Kuzyakov and Cheng, 2001, 2004; Dilkes et al., 2004; Heinemeyer et al., 2006, 2007; Moyano et al., 2007, 2008; Gaumont-Guay et al., 2008; Kuzyakov and Gavrichkova, 2010; Mahecha et al., 2010) are both derived from current photosynthate, and their respiratory rates couple closely with GPP. During the process of plant photosynthesis, growth respiration (R_g) consumes some photosynthate to provide energy for satisfying growth demand. At the same time, part of photosynthate is transferred into rhizosphere soil at high rate in the form of root exudates, which can be rapidly utilized by rhizosphere microorganisms (R_{rhi}) (Kuzyakov and Cheng, 2001, 2004; Dilkes et al., 2004; Kuzyakov and Gavrichkova, 2010). Thus, we defined the components of R_g and R_{rhi} as GPP-derived respiration (R_{GPP}), and assumed that R_{GPP} can be represented by a fraction of GPP (a).

$$R_{GPP} = R_g + R_{rhi} = a \times GPP \qquad (2)$$

The substrates for plant maintenance respiration (R_m) (Amthor, 2000; Chapin et al., 2011; Kuzyakov and Gavrichkova, 2010), microbial respiration of plant residues (R_{res}) (Waksman and Gerretsen, 1931; Zhou et al., 2013) and soil organic matter (SOM) decomposition (R_{SOM}) (Bader and Cheng, 2007; Heinemeyer et al., 2007; Moyano et al., 2007, 2008; Gaumont-Guay et al., 2008) are separately derived from plant biomass, plant residues and SOM, and their respiratory rates respond strongly to variation in temperature under no water-limited conditions. Since plant biomass, plant residues and SOM are the organic matters that are stored in the ecosystems over a long term period, we defined them as reserved ecosystem organic matter (EOM) and their corresponding respiratory components as EOM-derived respiration (R_{EOM}). If we assumed that the differences among the responses of R_m, R_{res} and R_{SOM} to the variation in temperature are negligible and employed the widely used Lloyd and Taylor model (Lloyd and Taylor, 1994) to represent the temperature effect, R_{EOM} can be expressed as follows:

$$R_{EOM} = R_m + R_{res} + R_{SOM} = R_{ref} \times e^{E_0*(1/(T_{ref}-T_0)-1/(T+273.15-T_0))}$$
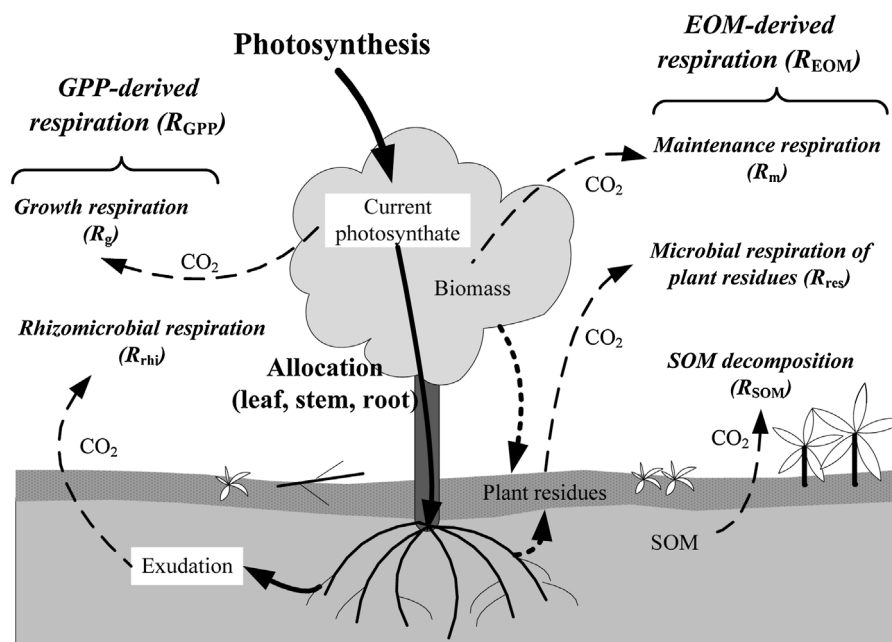$$(3)$$

Fig. 1. Components of ecosystem respiration. SOM, soil organic matter; EOM, reserved ecosystem organic matter, including plant biomass, plant residues and SOM.

where R_{ref} is the EOM-derived respiration (mol C m^{-2} d^{-1}) at the reference temperature, E_0 is the activation energy kind of parameter (K), T is temperature (°C), T_{ref} is the reference temperature, which is set to be 288.15 K (15 °C), T_0 is the minimum temperature for respiration, which is set to be 227.13 K (−46.02 °C).

Incorporating Eq. (2) with Eq. (3), we obtain a general form of the ReRSM as follows:

$$R_e = a \times GPP + R_{ref} \times e^{E_0 \times ((1/61.02)-(1/T+46.02))} \tag{4}$$

The second term in Eq. (4) is the EOM-derived respiration (R_{EOM}). While the study reported that the annual maximum LST (LST$_{max}$) from the Aqua/MODIS sensor increases faster than the site-observed maximum air temperature (T_{max}) as temperature increases (Mildrexler et al., 2011), the LST from the Terra/MODIS sensor was reported to correlate closely with the air temperature during daytime, nighttime and mean of the both (e.g., Sims et al., 2008; Ueyama et al., 2010). In our studied sites, the average of daytime LST and nighttime LST from the Terra/MODIS sensor also had a close relationship with the corresponding air temperature, with r^2 as high as to 0.91 and regression line approximating 1:1 line (Fig. S1). Since the purpose of this study was developing a totally satellite-driven R_e model and to keep the model more operationally, we use the average of daytime LST and nighttime LST from the Terra/MODIS sensor as a fist approximation of T in Eq. (4) in this version of the ReRSM. Then, R_{EOM} can be expressed as follows:

$$R_{EOM} = R_{ref} \times e^{E_0 \times ((1/61.02)-(1/LST+46.02))} \tag{5}$$

The first term in Eq. (4) is the GPP-derived respiration (R_{GPP}). We have developed a satellite-driven Photosynthetic Capacity Model (PCM) to estimate the dynamic change in GPP, which is solely driven by the Enhanced Vegetation Index (EVI) and the Land Surface Water Index (LSWI) (Gao et al., 2014).

$$GPP = PC_{max} \times EVI_s \times W_s \tag{6}$$

where PC$_{max}$ represents the maximum photosynthetic capacity (mol C m^{-2} d^{-1}) for each vegetation type or site, EVI$_s$ indicates the variability of photosynthetic capacity, the product of PC$_{max}$ and EVI$_s$ stands for the photosynthetic capacity (mol C m^{-2} d^{-1}), and W_s represents the water conditions which down-regulates the photosynthetic capacity. The values of EVI$_s$ and W_s are separately calculated from EVI and LSWI, and the detailed equations refer to Gao et al. (2014).

In this version of the ReRSM, we chose the PCM as a confident surrogate for GPP in Eq. (4), and R_{GPP} can be expressed as follows:

$$R_{GPP} = a \times PC_{max} \times EVI_s \times W_s \tag{7}$$

Merging Eq. (5) with Eq. (7), we can gain a solely satellite-driven R_e model:

$$R_e = a \times PC_{max} \times EVI_s \times W_s + R_{ref} \times e^{E_0 \times ((1/61.02)-(1/LST+46.02))} \tag{8}$$

Since soil moisture was reported to limit the rate of respiration at drought or severe drought regions through affecting the accessibility of respiratory substrate and the activity of relevant biological enzymes (Reichstein et al., 2002; Rey et al., 2002; Davidson and Janssens, 2006; Matías et al., 2012), we developed a variant of Eq. (8) with W_s multiplying the R_{EOM} part.

$$R_e = a \times PC_{max} \times EVI_s \times W_s + R_{ref} \times e^{E_0 \times ((1/61.02)-(1/LST+46.02))} \times W_s \tag{9}$$

The comparison showed that the estimated accuracy of Eq. (9) was nearly the same as Eq. (8) during either the whole year (Table S1) or the growing season (Table S2). Due to lack of a general equation in expressing the impact of soil moisture on R_e, we therefore chose Eq. (8) as the first version of the ReRSM. a, PC$_{max}$, R_{ref} and

E_0 are the model parameters, which expressed the variation of R_e across sites; EVI, LSWI and LST are the model variables, which indicated the temporal variation of R_e. The value of PC$_{max}$ in each vegetation type is derived from Gao et al. (2014). The theoretical assumptions and key equations related to the ReRSM are presented in Fig. 2.

2.2. Flux data

The eddy CO$_2$ flux data from the ChinaFLUX natural vegetation types located in Northern China and the Tibetan Plateau were chosen to assess the performance of the model in this study (Fig. 3). There are five vegetation types, including temperate mixed forest (the broad-leaved Korean pine mixed forest in the Changbai Mountains, MF), temperate steppe (STE), alpine shrubland (SHR), alpine marsh (MAR) and alpine meadow-steppe (MEA) (Table 1). The detailed information about the plant, soil and climate was introduced in the references at the last column.

Eddy covariance technique directly measures the net ecosystem CO$_2$ exchange (NEE) between ecosystem and the atmosphere. The observed half-hourly NEE values were processed in turns by three-dimensional coordinate rotation, WPL correction, storage correction (only for the forest site) and invalid data exclusion (Yu et al., 2006). We used the method introduced by Reichstein et al. (2005) to calculate ecosystem respiration. The valid nighttime NEE (i.e., nighttime R_e when the solar elevation angle <0) and soil temperature at 5 cm depth were chosen to fit the activation energy kind of parameter (E_0) for the Lloyd and Taylor model every five days using a 15-day moving window. Averaging the three E_0 with the smallest standard errors, we obtained the final E_0 for each site-year. Then, the reference respiration (R_{ref}) for the Lloyd and Taylor model was estimated every five days using a 10-day moving window. Based on the fitted model parameters (E_0 and R_{ref}) and soil temperature at 5 cm depth, the Lloyd and Taylor model was executed to calculate the daytime R_e and the missing nighttime R_e.

We summed the half-hourly R_e to obtain daily values, and the site-years with more than 20% of the daily R_e missing were STE in 2006, MAR in 2007 and SHR in 2009. To match the temporal resolution of the MODIS 8-day composite imagery, the daily R_e were further averaged within the same periods.

2.3. Remote sensing data

The MODIS data of EVI, LSWI and LST used in this study were downloaded from the University of Oklahoma Data Center [http://www.eomf.ou.edu/visualization/manual/], based on the pixels where the flux towers located (e.g., Xiao et al., 2004; Kalfas et al., 2011). The LST data is the average of daytime LST and nighttime LST. These data were all from the Terra/MODIS sensor and were 8-day composites. The spatial resolution of EVI and LSWI was 500 m, and of LST was 1 km.

2.4. Parameterization and validation

Multi-year eddy CO$_2$ flux observations of five vegetation types from ChinaFLUX were chosen for model parameterization and validation. The site-years with more than 20% of the observed daily R_e missing (i.e., STE in 2006, MAR in 2007 and SHR in 2009) were removed from both analyses. Model parameters (i.e., a, R_{ref} and E_0) were estimated using the nonlinear least squares (curve fitting) method with the trust-region-reflective optimization algorithm (Coleman and Li, 1996). Leave-one-out cross-validation was employed to validate the model, and the coefficient of determination (r^2), root mean square error (RMSE) and modeling efficiency (EF) were chosen to assess the performance of the model. The
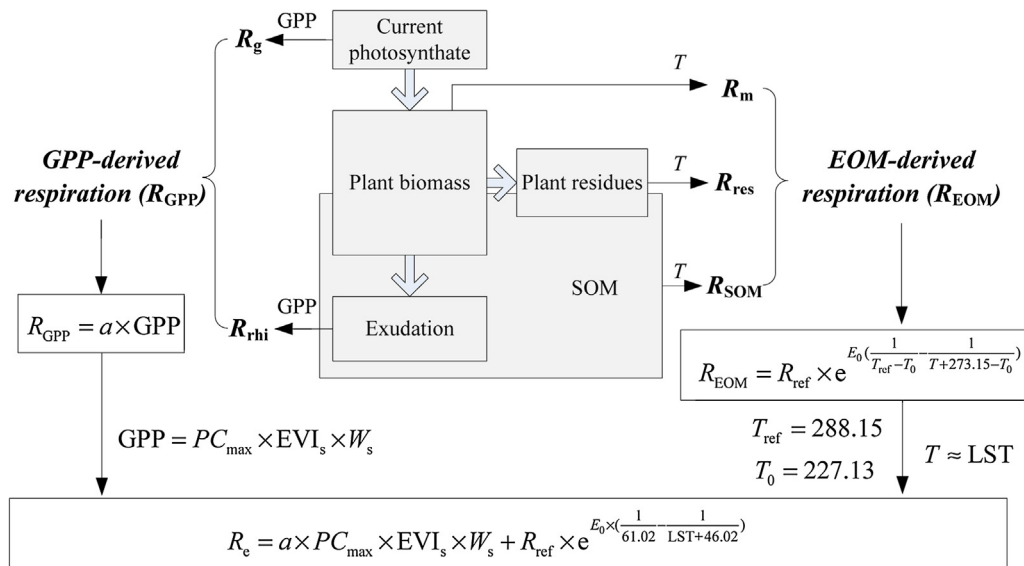
Fig. 2. Schematic diagram for the ReRSM. Description about the model parameters and variables refers to Table S3.

Table 1
A brief description of the five vegetation types.

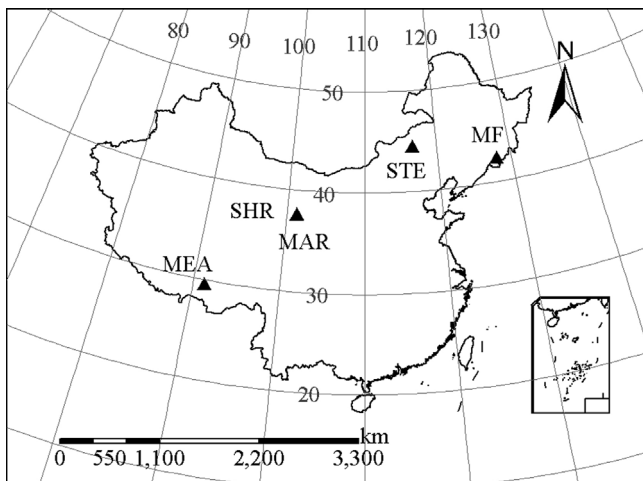| Code	Vegetation type	Latitude	Longitude	Site name	Mean annual temperature (°C)	Mean annual precipitation (mm)	Data period	Reference
MF	Temperate mixed forest	42.40	128.10	Changbaishan	0.9–4.0	600–810	2003–2008	Zhang et al. (2009)
STE	Temperate steppe	43.55	116.68	Inner Mongolia	−0.4	350.9	2004–2008	Wu et al. (2008)
SHR	Alpine shrubland	37.67	101.33	Haibei	−1.7	600	2004–2011	Li et al. (2007)
MAR	Alpine marsh	37.61	101.31	Haibei	−1.7	600	2004–2008	Li et al. (2007)
MEA	Alpine meadow-steppe	30.85	91.08	Damxung	1.3	480	2004–2009	Fu et al. (2009)

Fig. 3. Locations of the eddy-covariance towers in the five vegetation types. The flux towers at SHR and MAR locate in the same observation station. MF, temperate mixed forest; STE, temperate steppe; SHR, alpine shrubland; MAR, alpine marsh; and MEA, alpine meadow-steppe.

detailed introduction about the model validation and the statistics calculation can be found in Gao et al. (2014).

We chose a totally RS-driven R_e model, namely the RECO (Jägermeyr et al., 2014), to compare its ability in R_e estimation with that of the ReRSM in the studied five vegetation types. The RECO was conducted to estimate R_e in two ways in this study. The first is that the parameters related to the standardized respiration rate were re-fitted against the flux data for each vegetation type, while the reference respiration was directly derived from the observation due to the limited sites. The second is that all the parameters

of the RECO were derived from Jägermeyr et al. (2014). According to the standard of aggregated functional biome classification in the RECO, MF belonged to the Temperate and Humid Forests (TH FOR) and the T_{ref} was set to 12 °C, STE belonged to the Water-Limited Non-Forested Natural Vegetation (WL GRA/CRO) and the T_{ref} was set to 13 °C, and SHR, MAR and MEA belonged to the Temperature-Limited Non-Forested Natural Vegetation (TL GRA/CRO) and the T_{ref} was set to 0 °C. The r^2, RMSE and EF were chosen to assess the model performance.

Since the ReRSM parameters varied among the vegetations types, we analyzed their relationships with the mean annual growing season EVI (EVI_{sm}), LSWI ($LSWI_{sm}$), daytime LST ($LST_{dt, sm}$), nighttime LST ($LST_{nt, sm}$) and daily LST ($LST_{d, sm}$), and mean annual daytime LST ($LST_{dt, am}$), daily LST ($LST_{d, am}$) and nighttime $LST_{nt, am}$, respectively. The r^2 was chosen to assess their relationships.

3. Results

3.1. The ReRSM parameterization and validation

The long-term flux tower-observed R_e of five vegetation types were chosen for the ReRSM parameterization and validation. It required the missing daily R_e to be less than 20% in each site-year, and a total of 27 site-years met this requirement. The model parameterization showed that the ReRSM could explain approximately 74–94% of the variation in the observed R_e across five vegetation types, with the values of RMSE ranging from 0.02 to 0.06 mol C m^{-2} d^{-1} and EF ranging from 0.74 to 0.94 (Table 2). The cross-validation indicated that approximately 79–94% of the variation in the observed R_e over five vegetation types could be predicted by the ReRSM, with the values of RMSE varying from 0.02 to 0.06 mol C m^{-2} d^{-1} and EF varying from 0.65 to 0.93. According to

Table 2
Parameter estimates (a, PC_{max}, R_{ref} and E_0) and the coefficient of determination (r^2), root mean square error (RMSE), and modeling efficiency (EF) from the model parameterization and validation for each vegetation type. The values of PC_{max} were derived from Gao et al. (2014). MF, temperate mixed forest; STE, temperate steppe; SHR, alpine shrubland; MAR, alpine marsh; and MEA, alpine meadow-steppe.[a]

Site code	Parameterization							Validation		
	a	PC_{max} (mol C m^{-2} d^{-1})	R_{ref} (mol C m^{-2} d^{-1})	E_0 (K)	r^2	RMSE (mol C m^{-2} d^{-1})	EF	r^2	RMSE (mol C m^{-2} d^{-1})	EF
MF	0.27	2.61	0.27	267.30	0.93	0.06	0.93	0.94	0.06	0.92
STE	0.71	2.18	0.02	153.53	0.81	0.03	0.81	0.85	0.04	0.65
SHR	0.52	1.75	0.10	239.84	0.94	0.03	0.94	0.94	0.03	0.93
MAR	0.39	1.38	0.10	97.67	0.88	0.03	0.88	0.91	0.03	0.86
MEA	0.49	2.00	0.03	199.12	0.74	0.02	0.74	0.79	0.02	0.65

[a] There were differences between columns 6 (r^2) and 8 (EF), but these differences were too small to be shown in the table.

the statistics from both model parameterization and validation, the ReRSM performed best in SHR, followed by MF and MAR, while it performed a little low in STE and MEA. STE locates in the semi-arid region with a mean annual precipitation of only 350.9 mm and the precipitation distributed unevenly across seasons and years, which may be the main reason of the low performance in this vegetation type. The most likely reason for the low performance in MEA is its very sparse vegetation cover with the maximum leaf area index (LAI_{max}) of only 1.88 m^2 m^{-2} (Shi et al., 2006).

Further application of the ReRSM was based on the model parameters retrieved from the site-years with less than 20% of the daily R_e missing in each vegetation type to ensure the robust of the parameters (Table 2). The ReRSM was then executed to estimate all site-years R_e across five vegetation types (a total of 30 site-years, Table 1). Results showed that the ReRSM could explain approximately 93% of the variation in the flux tower-observed R_e, with the RMSE of 0.04 mol C m^{-2} d^{-1} and the EF of 0.93 (Fig. 4).

3.2. Seasonal and interannual dynamics of the ReRSM-estimated R_e

Using the model parameters in Table 2, the ReRSM was executed to estimate all 30 site-years R_e (Table 1) and then we compared the temporal dynamic in the ReRSM-estimated R_e with that in the flux tower-observed R_e (Fig. 5). In most cases, the estimated R_e is consistent with the observed R_e in terms of seasonal and interannual variation irrespective of vegetation types. The estimated maximal and minimal R_e separately matched closely with the corresponding observed R_e. The agreement in seasonality and magnitude of the estimated R_e vs. the observed R_e was best in SHR (Fig. 5c), followed by MF and MAR (Fig. 5a and d). However, in several 8-day periods, there were obvious gaps between the estimated R_e

Fig. 4. Comparison between the ReRSM-estimated R_e and the flux tower-observed R_e based on an 8-day average across five vegetation types.

and the observed R_e. For instance, the ReRSM underestimated the observed R_e at the peak growing season of 2006 in MF (Fig. 5a) and 2008 in STE (Fig. 5b). It was probably due to the influence of water stress on photosynthesis and respiration over this time period. The ReRSM also underestimated most of the observed R_e during 2007 in MAR (Fig. 5d). This site-year had limited observations, and the eddy covariance technique for flux observation and the data processing method may introduce errors into the flux tower-observed R_e.

3.3. Compare the performance of the ReRSM with that of the RECO

The statistics of the flux tower-observed R_e vs. RECO-estimated R_e were presented in Table 3. The RECO using the re-fitted parameters performed significantly better than using the original parameters. The values of the former RMSE and EF were respectively lower and higher than the latter ones by several orders of magnitude. When comparing the accuracy of the RECO model using the re-fitted parameters with that of the ReRSM from either parameterization or validation in Table 2, the performance of the ReRSM was comparable with that of the RECO in each vegetation type, especially in SHR and MEA. However, while the RECO had night parameters in water-limited sites and eight parameters in others, the ReRSM only had four parameters. These analyses indicated that the ReRSM is probably more appropriate in R_e estimation in our studied region.

3.4. Variations in the ReRSM parameters

The ReRSM parameters, i.e., a, PC_{max}, R_{ref} and E_0, differed among the vegetation types (Table 2). PC_{max} had been reported to correlate linearly with the mean annual nighttime LST ($LST_{nt, am}$, when the solar elevation angle <0, $r^2 = 0.86$, $p = 0.02$, Gao et al., 2014). We further analyzed the relationships of the other model parameters with the mean annual growing season EVI (EVI_{sm}), LSWI ($LSWI_{sm}$), daytime LST ($LST_{dt, sm}$), nighttime LST ($LST_{nt, sm}$) and daily LST ($LST_{d, sm}$), and mean annual daytime LST ($LST_{dt, am}$), daily LST ($LST_{d, am}$) and nighttime $LST_{nt, am}$, it revealed that E_0 correlated insignificantly with any of the above satellite-derived indices. a showed a negative linear relationship with $LSWI_{sm}$ (Fig. 6a), and R_{ref} showed positive linear relationships with both EVI_{sm} ($r^2 = 0.84$, $p = 0.03$) and $LSWI_{sm}$ (Fig. 6b), with the r^2 of R_{ref} vs. $LSWI_{sm}$ higher than that of R_{ref} vs. EVI_{sm}.

4. Discussions

4.1. Biological basis of the ReRSM

This study developed a solely satellite-driven R_e model (ReRSM) by assuming that ecosystem respiration (R_e) can be separated into GPP-derived respiration (R_{GPP}) and EOM-derived respiration (R_{EOM}). The ReRSM performed well in R_e estimation across five
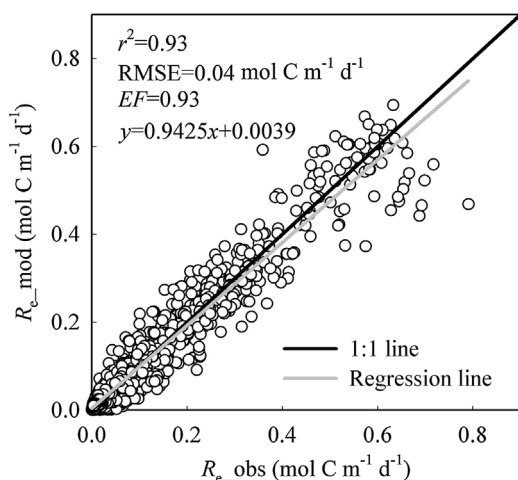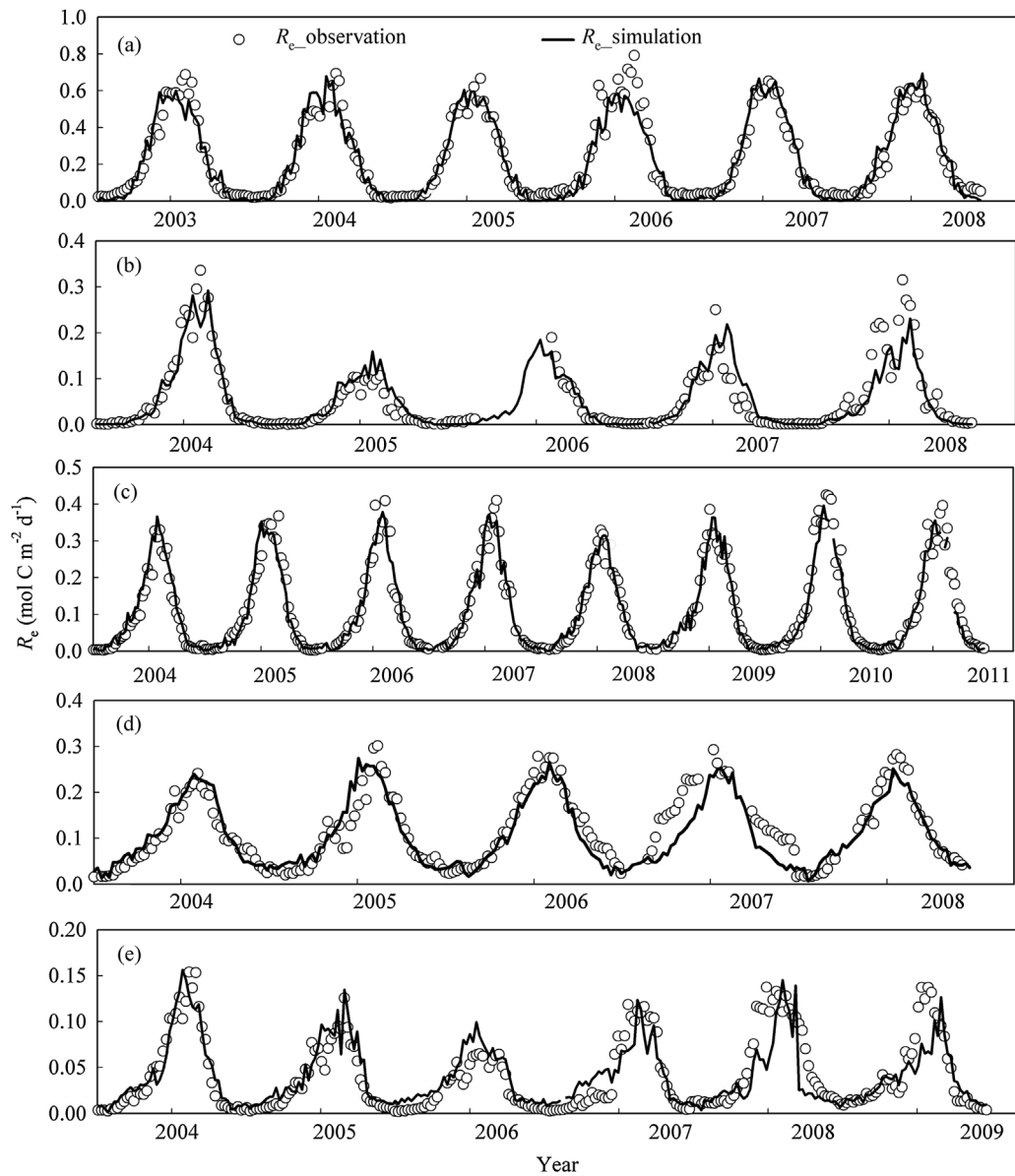
Fig. 5. The seasonal and interannual variation in the ReRSM-estimated R_e vs. the flux tower-observed R_e, based on an 8-day average. The white circles represent the flux tower-observed R_e, while the black lines represent the ReRSM-estimated R_e. (a) temperate mixed forest (MF); (b) temperate steppe (STE); (c) alpine shrubland (SHR); (d) alpine marsh (MAR); and (e) alpine meadow-steppe (MEA).

Table 3
The statistics of the RECO-estimated R_e vs. flux tower-observed R_e for each vegetation type. MF, temperate mixed forest; STE, temperate steppe; SHR, alpine shrubland; MAR, alpine marsh; and MEA, alpine meadow-steppe. TH FOR, Temperate and Humid Forests; WL GRA/CRO, Water-Limited Non-Forested Natural Vegetation; and TL GRA/CRO, Temperature-Limited Non-Forested Natural Vegetation.

Code	Aggregated functional biomes	T_{ref} (°C)	RECO[a]			RECO[b]		
			r^2	RMSE (mol C m^{-2} d^{-1})	EF	r^2	RMSE (mol C m^{-2} d^{-1})	EF
MF	TH FOR	12	0.87	0.08	0.86	0.88	0.20	0.17
STE	WL GRA/CRO	13	0.66	0.05	0.63	0.60	0.10	−0.84
SHR	TL GRA/CRO	0	0.78	0.06	0.78	0.56	0.13	−0.16
MAR	TL GRA/CRO	0	0.83	0.03	0.83	0.60	0.11	−0.98
MEA	TL GRA/CRO	0	0.46	0.03	0.30	0.02	0.06	−1.01

[a] The parameters related to the standardized respiration rate in the RECO were re-fitted against the flux data for each vegetation type, while the reference respiration in the RECO was directly derived from the observation due to the limited sites.
[b] All the parameters of the RECO were derived from Jägermeyr et al. (2014).

vegetation types (Table 2, Fig. 4), and clearly described the seasonal and interannual dynamics in the flux tower-observed R_e (Fig. 5).

The GPP-derived respiration in the ReRSM includes growth respiration (R_g) and rhizomicrobial respiration (R_{rhi}). The ReRSM

employed a fraction of GPP to represent the dynamic change in R_{GPP}, which is decided by the mechanisms behind photosynthesis and respiration. Plant photosynthesis and the process of storing the current photosynthate into its various organs necessarily need
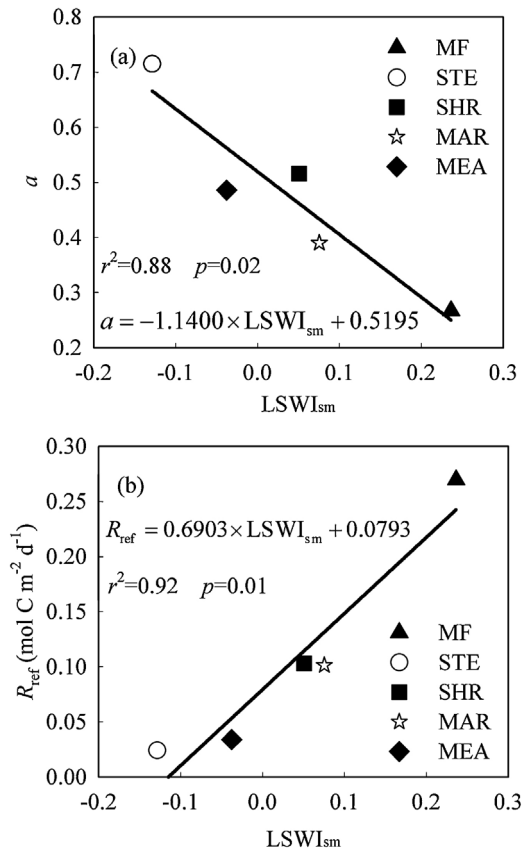
Fig. 6. The relationships (a) between a and $LSWI_{sm}$ and (b) between R_{ref} and $LSWI_{sm}$. $LSWI_{sm}$, mean annual LSWI within the growing season. MF, temperate mixed forest; STE, temperate steppe; SHR, alpine shrubland; MAR, alpine marsh; and MEA, alpine meadow-steppe.

energy supply from growth respiration at the cost of consuming some photosynthate. R_g is always a nearly constant fraction of net primary production or GPP under any environmental conditions (Amthor, 2000; Chapin et al., 2011; Piao et al., 2010). Meanwhile, part of current photosynthate is transported into roots to sustain their physiological function and then released into the rhizosphere soil in the form of root exudates. Root exudates are characteristic of low molecular weight and labile organic matter, which serve as the substrates for R_{rhi} and can be rapidly respired by microorganisms in the rhizosphere. This is because available substances are the actual contributors to microbial activity (Kuzyakov and Gavrichkova, 2010), and thus rhizosphere microorganisms can be activated rapidly in the presence of root exudates (Chapin et al., 2011; Huang et al., 2012). Some studies have reported that there is a time lag between GPP and respiration response from the soil. The time lag was approximately 12.5 ± 7.5 (SD) h in grasses, 1–2 days in crops, and 4–5 days in mature trees (Knohl et al., 2005; Moyano et al., 2008; Kuzyakov and Gavrichkova, 2010). Because the ReRSM was conducted at the temporal resolution of 8-day average, these kinds of time lag may introduce negligible error into the ReRSM-estimated R_e. Although the studies sometimes observed a link between GPP-derived respiration and temperature (Moyano et al., 2007, 2008), it is to a large extent due to the good relationship between GPP and temperature (Amthor, 2000; Chapin et al., 2011; Kuzyakov and Gavrichkova, 2010; Huang et al., 2012).

The EOM-derived respiration in the ReRSM includes maintenance respiration (R_m), microbial respiration of plant residues (R_{res}) and SOM decomposition (R_{SOM}), with the respiratory substrates derived from plant biomass, plant residues and SOM, respectively. The ReRSM chose the Lloyd and Taylor model to represent the R_{EOM}

dynamic by assuming a same response of R_m, R_{res} and R_{SOM} to variation in temperature. Strictly speaking, there should be some differences among the responses due to different characteristics of their substrates. However, it was very difficult to partition these differences based on either ground observations or remote sensing data, and an excessive number of model parameters or variables also limited model application at regional scale. It was reported that there are necessarily functional linkages among plant biomass, plant residues and SOM. SOM correlates closely with soil quality (Reeves, 1997; Al-Kaisi et al., 2005), which influences plant available nutrients and the ability of soil in absorbing plant nutrients (Chen et al., 2005; Ladoni et al., 2010). Both of them primarily determine plant photosynthetic capacity (Chapin et al., 2011; Janssens et al., 2001) and plant biomass over long term periods. Plant species with high productivity are characterized by high quality of residues and high rate of residues decomposition (Chapin et al., 2011; De Deyn et al., 2008). Therefore, it was feasible to assume the identical response of R_m, R_{res} and R_{SOM} to variation in temperature, and the high accuracy of the ReRSM in R_e estimation across five vegetation types also supported this simplification.

4.2. Characteristics of the model parameters

The ReRSM had four model parameters, i.e., a, PC_{max}, R_{ref} and E_0, all of which varied among vegetation types due to different vegetation structures, site conditions and histories (Table 2). PC_{max} indicated the maximum photosynthetic capacity, which correlated significantly with the mean annual nighttime LST ($LST_{nt, am}$), with the r^2 of 0.86 (Gao et al., 2014). It may be because $LST_{n, am}$ is a good indicator of the baseline temperature that decides plant phenology (Sims et al., 2008).

R_{ref} represented the EOM-derived respiration at the reference temperature. The substrates for R_{EOM} included plant biomass, plant residues and SOM. They are all related to the long-term plant productivity as discussed above. Photosynthesis is mainly decided by canopy chlorophyll content and water conditions (Gao et al., 2014), which can be represented by EVI and LSWI, respectively. R_{ref} was thus found to show significantly positive relationships with both mean annual growing season EVI (EVI_{sm}) and LSWI ($LSWI_{sm}$), with the r^2 of 0.84 and 0.92, respectively (Fig. 6b). Previous studies also indicated that reference respiration depends strongly on mean annual GPP (e.g., Yuan et al., 2011), and can be estimated by LAI_{max} (e.g., Migliavacca et al., 2011) or mean annual springtime EVI (e.g., Jägermeyr et al., 2014).

a was a fraction of GPP that is transformed into GPP-derived respiration. It was observed that a shows a significantly negative relationship with $LSWI_{sm}$, with the r^2 of 0.88 (Fig. 6a). $LSWI_{sm}$ represented the mean annual water conditions within the growing season, which is a main environmental factor in determining plant photosynthesis. The negative relationship between a and $LSWI_{sm}$ may be because the plants with more water content tend to produce higher GPP and convert lower current photosynthate into GPP-derived respiration. However, the mechanisms under this relationship still need a further study.

E_0 was the activation energy kind of parameter, which can be used to represent the temperature sensitivity of respiration. There was no significant relationship between E_0 and any of the mean annual satellite-derived indices related to canopy greenness, water and temperature over either growing season or whole year. The question if the temperature sensitivity of respiration varies over time and among vegetation types is still under debate (Davidson and Janssens, 2006; Mahecha et al., 2010; Chen et al., 2010; Yvon-Durocher et al., 2012; Jägermeyr et al., 2014). Although many evidences showed that E_0 varies among compounds and decomposition of labile SOM has lower temperature sensitivity than decomposition of recalcitrant SOM (Davidson and Janssens,
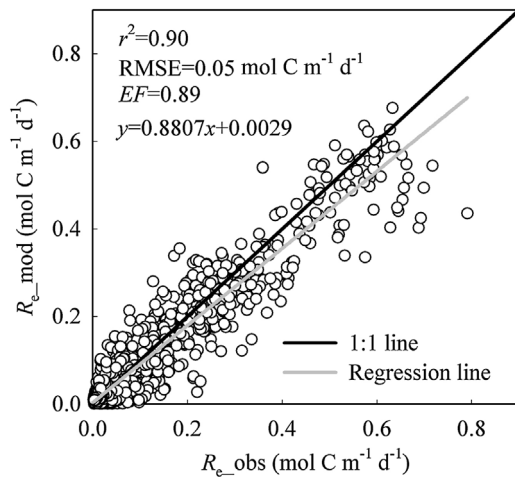
Fig. 7. Comparison between the ReRSM-estimated R_e and the flux tower-observed R_e based on an 8-day average across five vegetation types. The model parameters of the ReRSM were separately calculated from Eqs. (10)–(12).

2006), some researches reported that temperature sensitivities of respiration are remarkably similar among ecosystems (Yvon-Durocher et al., 2012), and can be even considered as a constant (Mahecha et al., 2010). If we assumed that E_0 is a constant of 308.56 K for different vegetation types (termed E_0') according to Lloyd and Taylor, (1994), the re-parameterized and re-validated statistics of the ReRSM were almost the same as those in Table 2, except the values of EF in MAR dropped separately from 0.88 and 0.86 to 0.78 and 0.76. The re-fitted model parameters of a (termed a') and R_{ref} (termed R_{ref}') still correlated respectively negatively ($r^2 = 0.88$, $p = 0.02$) and positively ($r^2 = 0.96$, $p < 0.01$) with $LSWI_{sm}$. We chose a_{GPP}' to represent the product of α' and PC_{max}. If PC_{max} was represented by the linear function of $LST_{n, am}$ (Gao et al., 2014), the model parameters of a_{GPP}', R_{ref}' and E_0' can be separately expressed as follows:

$$a_{GPP}' = (-1.2759 \times LSWI_{sm} + 0.5079)$$
$$\times (0.1346 \times LST_{n\_am} + 2.7522) \qquad (10)$$

$$R_{ref}' = 0.7566 \times LSWI_{sm} + 0.0874 \qquad (11)$$

$$E_0' = 308.56 \qquad (12)$$

When using the model parameters that were calculated from Eqs. (10)–(12), the ReRSM can explain approximately 90% of the variation in the observed R_e across five vegetation types, with the RMSE of 0.05 mol C m^{-2} d^{-1} and the EF of 0.89 (Fig. 7). This result suggests the potential application of the ReRSM in estimating spatial variability of R_e. However, the slope of the regression line in Fig. 7 was smaller than that in Fig. 4, which resulted in the obvious R_e underestimation in Fig. 7, especially at the higher R_e values. This was primarily due to the differences between the fitted parameters and the ones that were calculated from Eqs. (10)–(12). Furthermore, R_e is affected by a series of biological, physical and chemical processes and their interactions, which are currently not well understood (Jägermeyr et al., 2014), and therefore not being included in the model. In the further study, more factors that possibly affect the value of the model parameters should be explicitly analyzed.

4.3. Model applications and limitations

The ReRSM has the clear biological basis, and performed well in R_e estimation across five vegetation types in Northern China and the Tibetan Plateau. The model is only driven by the MODIS-retrieved EVI, LSWI and LST, which facilitates the use of the ReRSM at high temporal and spatial resolution. Model comparison showed that the accuracy of the ReRSM, which had much fewer parameters, was comparable with that of the RECO in the studied five vegetation types. The ReRSM parameters also showed close relationships with the mean annual satellite-derived indices, i.e., Eqs. (10)–(12). These results indicated that the ReRSM has the potential to estimate spatially distributed R_e. However, the further application of the ReRSM at regional or global scale probably has several limitations.

(1) The ReRSM probably provides poor R_e estimates under severe drought conditions because it did not contain the effect of moisture on R_e. (2) The ReRSM may be incapable of estimating the pulse increase of R_e when high plant residues occur, because it did not consider the dynamic of plant residues. (3) The value of R_e was also influenced by amounts of other biotic and abiotic factors, such as nutrient availability (Fernández-Martínez et al., 2014), age of the ecosystem (Piao et al., 2010; Fernández-Martínez et al., 2014), disturbance and acclimation effects. Although the satellite-derived indices of EVI and LSWI to some extent can reflect these impacts on GPP-derived respiration, they are difficult to mirror the influences on EOM-derived respiration. Thus, more factors related to R_e should be analyzed and effectively presented in the model, and the ReRSM is only the first step of building a totally satellite-driven R_e model. Its performance in other vegetation types or regions needs to be validated in further study. Along with the development of satellite algorithms about soil moisture, plant biomass, nutrient availability, human activity, and so on, we will optimize the model structure to improve its accuracy.

Appendix A. Supplementary data

Supplementary data associated with this article can be found, in the online version, at http://dx.doi.org/10.1016/j.ecolmodel.2015.03.001.

References

Al-Kaisi, M.M., Yin, X., Licht, M.A., 2005. Soil carbon and nitrogen changes as influenced by tillage and cropping systems in some Iowa soils. Agric. Ecosyst. Environ. 105, 635–647.

Amthor, J.S., 2000. The McCree–de Wit–Penning de Vries–Thornley respiration paradigms: 30 years later. Ann. Bot. 86, 1–20.

Bader, N.E., Cheng, W., 2007. Rhizosphere priming effect of *Populus fremontii* obscures the temperature sensitivity of soil organic carbon respiration. Soil Biol. Biochem. 39, 600–606.

Bahn, M., Rodeghiero, M., Anderson-Dunn, M., Dore, S., Gimeno, C., Drösler, M., Williams, M., Ammann, C., Berninger, F., Flechard, C., Jones, S., Balzarolo, M., Kumar, S., Newesely, C., Priwitzer, T., Raschi, A., Siegwolf, R., Susiluoto, S., Tenhunen, J., Wohlfahrt, G., Cernusca, A., 2008. Soil respiration in European grasslands in relation to climate and assimilate supply. Ecosystems 11, 1352–1367.

Bond-Lamberty, B., Thomson, A., 2010. Temperature-associated increases in the global soil respiration record. Nature 464, 579–582.

Chapin III, F.S., Matson, P.A., Vitousek, P.M., 2011. Principles of Terrestrial Ecosystem Ecology, 2nd ed. Springer Science + Business Media, New York.

Chen, F., Kissel, D.E., West, L.T., Rickman, D., Luvall, J.C., Adkins, W., 2005. Mapping surface soil organic carbon for crop fields with remote sensing. J. Soil Water Conserv. 60, 51–57.

Chen, S., Huang, Y., Zou, J., Shen, Q., Hu, Z., Qin, Y., Chen, H., Pan, G., 2010. Modeling interannual variability of global soil respiration from climate and soil properties. Agric. For. Meteorol. 150, 590–605.

Coleman, T.F., Li, Y., 1996. An interior, trust region approach for nonlinear minimization subject to bounds. SIAM J. Optim. 6, 418–445.

Davidson, E.A., Janssens, I.A., 2006. Temperature sensitivity of soil carbon decomposition and feedbacks to climate change. Nature 440, 165–173.

De Deyn, G.B., Cornelissen, J.H.C., Bardgett, R.D., 2008. Plant functional traits and soil carbon sequestration in contrasting biomes. Ecol. Lett. 11, 516–531.

Dilkes, N.B., Jones, D.L., Farrar, J., 2004. Temporal dynamics of carbon partitioning and rhizodeposition in wheat. Plant Physiol. 134, 706–715.

Fernández-Martínez, M., Vicca, S., Janssens, I.A., Sardans, J., Luyssaert, S., Campioli, M., Chapin III, F.S., Ciais, P., Malhi, Y., Obersteiner, M., Papale, D., Piao, S., Reichstein, M., Rodà, F., Peñuelas, J., 2014. Nutrient availability as the key regulator of global forest carbon balance. Nat. Clim. Chang. 4, 471–476.

Frank, A.B., Liebig, M.A., Hanson, J.D., 2002. Soil carbon dioxide fluxes in northern semiarid grasslands. Soil Biol. Biochem. 34, 1235–1241.

Fu, Y., Zheng, Z., Yu, G., Hu, Z., Sun, X., Shi, P., Wang, Y., Zhao, X., 2009. Environmental influences on carbon dioxide fluxes over three grassland ecosystems in China. Biogeosciences 6, 2879–2893.

Gao, Y., Yu, G., Yan, H., Zhu, X., Li, S., Wang, Q., Zhang, J., Wang, Y., Li, Y., Zhao, L., Shi, P., 2014. A MODIS-based Photosynthetic Capacity Model to estimate gross primary production in Northern China and the Tibetan Plateau. Remote Sens. Environ. 148, 108–118.

Gaumont-Guay, D., Black, T.A., Barr, A.G., Jassal, R.S., Nesic, Z., 2008. Biophysical controls on rhizospheric and heterotrophic components of soil respiration in a boreal black spruce stand. Tree Physiol. 28, 161–171.

Gilmanov, T.G., Tieszen, L.L., Wylie, B.K., Flanagan, L.B., Frank, A.B., Haferkamp, M.R., Meyers, T.P., Morgan, J.A., 2005. Integration of CO$_2$ flux and remotely-sensed data for primary production and ecosystem respiration analyses in the Northern Great Plains: potential for quantitative spatial extrapolation. Glob. Ecol. Biogeogr. 14, 271–292.

Gitelson, A.A., Viña, A., Verma, S.B., Rundquist, D.C., Arkebauer, T.J., Keydan, G., Leavitt, B., Ciganda, V., Burba, G.G., Suyker, A.E., 2006. Relationship between gross primary production and chlorophyll content in crops: implications for the synoptic monitoring of vegetation productivity. J. Geophys. Res. Atmos. 111, D08S11, http://dx.doi.org/10.1029/2005JD006017.

Gitelson, A.A., Peng, Y., Masek, J.G., Rundquist, D.C., Verma, S., Suyker, A., Baker, J.M., Hatfield, J.L., Meyers, T., 2012. Remote estimation of crop gross primary production with Landsat data. Remote Sens. Environ. 121, 404–414.

Gomez-Casanovas, N., Matamala, R., Cook, D.R., Gonzalez-Meler, M.A., 2012. Net ecosystem exchange modifies the relationship between the autotrophic and heterotrophic components of soil respiration with abiotic factors in prairie grasslands. Glob. Chang. Biol. 18, 2532–2545.

Heinemeyer, A., Ineson, P., Ostle, N., Fitter, A., 2006. Respiration of the external mycelium in the arbuscular mycorrhizal symbiosis shows strong dependence on recent photosynthates and acclimation to temperature. New Phytol. 171, 159–170.

Heinemeyer, A., Hartley, I.P., Evans, S.P., Carreira De La Fuente, J.A., Ineson, P., 2007. Forest soil CO$_2$ flux: uncovering the contribution and environmental responses of ectomycorrhizas. Glob. Chang. Biol. 13, 1786–1797.

Huang, N., Niu, Z., 2013. Estimating soil respiration using spectral vegetation indices and abiotic factors in irrigated and rainfed agroecosystems. Plant Soil 367, 535–550.

Huang, N., Niu, Z., Zhan, Y., Xu, S., Tappert, M.C., Wu, C., Huang, W., Gao, S., Hou, X., Cai, D., 2012. Relationships between soil respiration and photosynthesis-related spectral vegetation indices in two cropland ecosystems. Agric. For. Meteorol. 160, 80–89.

Jägermeyr, J., Gerten, D., Lucht, W., Hostert, P., Migliavacca, M., Nemani, R., 2014. A high-resolution approach to estimating ecosystem respiration at continental scales using operational satellite data. Glob. Chang. Biol. 20, 1191–1210.

Janssens, I.A., Lankreijer, H., Matteucci, G., Kowalski, A.S., Buchmann, N., Epron, D., Pilegaard, K., Kutsch, W., Longdoz, B., Grünwald, T., Montagnani, L., Dore, S., Rebmann, C., Moors, E.J., Grelle, A., Rannik, Ü., Morgenstern, K., Oltchev, S., Clement, R., Guðmundsson, J., Minerbi, S., Berbigier, P., Ibrom, A., Moncrieff, J., Aubinet, M., Bernhofer, C., Jensen, N.O., Vesala, T., Granier, A., Schulze, E.D., Lindroth, A., Dolman, A.J., Jarvis, P.G., Ceulemans, R., Valentini, R., 2001. Productivity overshadows temperature in determining soil and ecosystem respiration across European forests. Glob. Chang. Biol. 7, 269–278.

Kalfas, J.L., Xiao, X., Vanegas, D.X., Verma, S.B., Suyker, A.E., 2011. Modeling gross primary production of irrigated and rain-fed maize using MODIS imagery and CO$_2$ flux tower data. Agric. For. Meteorol. 151, 1514–1528.

Knohl, A., Werner, R.A., Brand, W.A., Buchmann, N., 2005. Short-term variations in δ^{13}C of ecosystem respiration reveals link between assimilation and respiration in a deciduous forest. Oecologia 142, 70–82.

Kuzyakov, Y., Cheng, W., 2001. Photosynthesis controls of rhizosphere respiration and organic matter decomposition. Soil Biol. Biochem. 33, 1915–1925.

Kuzyakov, Y., Cheng, W., 2004. Photosynthesis controls of CO$_2$ efflux from maize rhizosphere. Plant Soil 263, 85–99.

Kuzyakov, Y., Gavrichkova, O., 2010. Review: Time lag between photosynthesis and carbon dioxide efflux from soil: a review of mechanisms and controls. Glob. Chang. Biol. 16, 3386–3406.

Ladoni, M., Bahrami, H.A., Alavipanah, S.K., Norouzi, A.A., 2010. Estimating soil organic carbon from soil reflectance: a review. Precis. Agric. 11, 82–99.

Larsen, K.S., Ibrom, A., Beier, C., Jonasson, S., Michelsen, A., 2007. Ecosystem respiration depends strongly on photosynthesis in a temperate heath. Biogeochemistry 85, 201–213.

Li, Z., Yu, G., Xiao, X., Li, Y., Zhao, X., Ren, C., Zhang, L., Fu, Y., 2007. Modeling gross primary production of alpine ecosystems in the Tibetan Plateau using MODIS images and climate data. Remote Sens. Environ. 107, 510–519.

Lloyd, J., Taylor, J.A., 1994. On the temperature dependence of soil respiration. Funct. Ecol. 8, 315–323.

Mahecha, M.D., Reichstein, M., Carvalhais, N., Lasslop, G., Lange, H., Seneviratne, S.I., Vargas, R., Ammann, C., Arain, M.A., Cescatti, A., Janssens, I.A., Migliavacca, M., Montagnani, L., Richardson, A.D., 2010. Global convergence in the temperature sensitivity of respiration at ecosystem level. Science 329, 838–840.

Matías, L., Castro, J., Zamora, R., 2012. Effect of simulated climate change on soil respiration in a Mediterranean-type ecosystem: rainfall and habitat type are more important than temperature or the soil carbon pool. Ecosystems 15, 299–310.

Migliavacca, M., Reichstein, M., Richardson, A.D., Colombo, R., Sutton, M.A., Lasslop, G., Tomelleri, E., Wohlfahrt, G., Carvalhais, N., Cescatti, A., Mahecha, M.D., Montagnani, L., Papale, D., Zaehle, S., Arain, A., Arneth, A., Black, T.A., Carrara, A., Dore, S., Gianelle, D., Helfter, C., Hollinger, D., Kutsch, W.L., Lafleur, P.M., Nouvellon, Y., Rebmann, C., Da Rocha, H.R., Rodeghiero, M., Roupsard, O., SebastiÀ, M.-T., Seufert, G., Soussana, J.-F., Van Der Molen, M.K., 2011. Semiempirical modeling of abiotic and biotic factors controlling ecosystem respiration across eddy covariance sites. Glob. Chang. Biol. 17, 390–409.

Mildrexler, D.J., Zhao, M., Running, S.W., 2011. A global comparison between station air temperatures and MODIS land surface temperatures reveals the cooling role of forests. J. Geophys. Res. 116, G03025, http://dx.doi.org/10.1029/2010JG001486.

Moyano, F.E., Kutsch, W.L., Schulze, E.-D., 2007. Response of mycorrhizal, rhizosphere and soil basal respiration to temperature and photosynthesis in a barley field. Soil Biol. Biochem. 39, 843–853.

Moyano, F.E., Kutsch, W.L., Rebmann, C., 2008. Soil respiration fluxes in relation to photosynthetic activity in broad-leaf and needle-leaf forest stands. Agric. For. Meteorol. 148, 135–143.

Olofsson, P., Lagergren, F., Lindroth, A., Lindström, J., Klemedtsson, L., Kutsch, W., Eklundh, L., 2008. Towards operational remote sensing of forest carbon balance across Northern Europe. Biogeosciences 5, 817–832.

Piao, S., Luyssaert, S., Ciais, P., Janssens, I.A., Chen, A., Cao, C., Fang, J., Friedlingstein, P., Luo, Y., Wang, S., 2010. Forest annual carbon cost: a global-scale analysis of autotrophic respiration. Ecology 91, 652–661.

Rahman, A.F., Sims, D.A., Cordova, V.D., EI-Masri, B.Z., 2005. Potential of MODIS EVI and surface temperature for directly estimating per-pixel ecosystem C fluxes. Geophys. Res. Lett. 32, L19404, http://dx.doi.org/10.1029/2005GL024127.

Reeves, D.W., 1997. The role of soil organic matter in maintaining soil quality in continuous cropping systems. Soil Tillage Res. 43, 131–167.

Reichstein, M., Tenhunen, J.D., Roupsard, O., Ourcival, J.M., Rambal, S., Dore, S., Valentini, R., 2002. Ecosystem respiration in two Mediterranean evergreen Holm Oak forests: drought effects and decomposition dynamics. Funct. Ecol. 16, 27–39.

Reichstein, M., Rey, A., Freibauer, A., Tenhunen, J., Valentini, R., Banza, J., Casals, P., Cheng, Y., Grünzweig, J.M., Irvine, J., Joffre, R., Law, B.E., Loustau, D., Miglietta, F., Oechel, W., Ourcival, J.-M., Pereira, J.S., Peressotti, A., Ponti, F., Qi, Y., Rambal, S., Rayment, M., Romanya, J., Rossi, F., Tedeschi, V., Tirone, G., Xu, M., Yakir, D., 2003. Modeling temporal and large-scale spatial variability of soil respiration from soil water availability, temperature and vegetation productivity indices. Glob. Biogeochem. Cycles 17, 1104, http://dx.doi.org/10.1029/2003GB002035.

Reichstein, M., Falge, E., Baldocchi, D., Papale, D., Aubinet, M., Berbigier, P., Bernhofer, C., Buchmann, N., Gilmanov, T., Granier, A., Grünwald, T., Havránková, K., Ilvesniemi, H., Janous, D., Knohl, A., Laurila, T., Lohila, A., Loustau, D., Matteucci, G., Meyers, T., Miglietta, F., Ourcival, J.-M., Pumpanen, J., Rambal, S., Rotenberg, E., Sanz, M., Tenhunen, J., Seufert, G., Vaccari, F., Vesala, T., Yakir, D., Valentini, R., 2005. On the separation of net ecosystem exchange into assimilation and ecosystem respiration: review and improved algorithm. Glob. Chang. Biol. 11, 1424–1439.

Rey, A., Pegoraro, E., Tedeschi, V., De Parri, I., Jarvis, P.G., Valentini, R., 2002. Annual variation in soil respiration and its components in a coppice oak forest in Central Italy. Glob. Chang. Biol. 8, 851–866.

Running, S.W., Nemani, R.R., Heinsch, F.A., Zhao, M., Reeves, M., Hashimoto, H., 2004. A continuous satellite-derived measure of global terrestrial primary production. Bioscience 54, 547–560.

Schubert, P., Eklundh, L., Lund, M., Nilsson, M., 2010. Estimating northern peatland CO$_2$ exchange from MODIS time series data. Remote Sens. Environ. 114, 1178–1189.

Shi, P., Sun, X., Xu, L., Zhang, X., He, Y., Zhang, D., Yu, G., 2006. Net ecosystem CO$_2$ exchange and controlling factors in a steppe-Kobresia meadow on the Tibetan Plateau. Sci. China Ser. D: Earth Sci. 49 (Supp. II), 207–218.

Sims, D.A., Rahman, A.F., Cordova, V.D., El-Masri, B.Z., Baldocchi, D.D., Bolstad, P.V., Flanagan, L.B., Goldstein, A.H., Hollinger, D.Y., Misson, L., Monson, R.K., Oechel, W.C., Schmid, H.P., Wofsy, S.C., Xu, L., 2008. A new model of gross primary productivity for North American ecosystems based solely on the enhanced vegetation index and land surface temperature from MODIS. Remote Sens. Environ. 112, 1633–1646.

Tang, J., Baldocchi, D.D., Xu, L., 2005. Tree photosynthesis modulates soil respiration on a diurnal time scale. Glob. Chang. Biol. 11, 1298–1304.

Tang, X., Wang, Z., Liu, D., Song, K., Jia, M., Dong, Z., Munger, J.W., Hollinger, D.Y., Bolstad, P.V., Goldstein, A.H., Desai, A.R., Dragoni, D., Liu, X., 2012. Estimating the net ecosystem exchange for the major forests in the northern United States by integrating MODIS and AmeriFlux data. Agric. For. Meteorol. 156, 75–84.

Trumbore, S., 2006. Carbon respired by terrestrial ecosystems – recent progress and challenges. Glob. Chang. Biol. 12, 141–153.

Ueyama, M., Harazono, Y., Ichii, K., 2010. Satellite-based modeling of the carbon fluxes in mature black spruce forests in Alaska: a synthesis of the eddy covariance data and satellite remote sensing data. Earth Interact., 14, http://dx.doi.org/10.1175/2010EI319.1.

Valentini, R., Matteucci, G., Dolman, A.J., Schulze, E.D., Rebmann, C., Moors, E.J., Granier, A., Gross, P., Jensen, N.O., Pilegaard, K., Lindroth, A., Grelle, A., Bernhofer, C., Grünwald, T., Aubinet, M., Ceulemans, R., Kowalski, A.S., Vesala, T., Rannik, Ü., Berbigier, P., Loustau, D., Gudmundsson, J., Thorgeirsson, H., Ibrom, A., Morgenstern, K., Clement, R., Moncrieff, J., Montagnani, L., Minerbi, S., Jarvis, P.G., 2000. Respiration as the main determinant of carbon balance in European forests. Nature 404, 861–865.

Vourlitis, G.L., Verfaillie, J., Oechel, W.C., Hope, A., Stow, D., Engstrom, R., 2003. Spatial variation in regional CO$_2$ exchange for the Kuparuk River Basin. Alaska over the summer growing season. Glob. Chang. Biol. 9, 930–941.

Waksman, S.A., Gerretsen, F.C., 1931. Influence of temperature and moisture upon the nature and extent of decomposition of plant residues by microorganisms. Ecology 12, 33–60.

Wu, W., Wang, S., Xiao, X., Yu, G., Fu, Y., Hao, Y., 2008. Modeling gross primary production of a temperate grassland ecosystem in Inner Mongolia, China, using MODIS imagery and climate data. Sci. China Ser. D: Earth Sci. 51, 1501–1512.

Wu, C., Niu, Z., Gao, S., 2010. Gross primary production estimation from MODIS data with vegetation index and photosynthetically active radiation in maize. J. Geophys. Res. Atmos. 115, D12127, http://dx.doi.org/10.1029/2009JD013023.

Xiao, X., Hollinger, D., Aber, J., Goltz, M., Davidson, E.A., Zhang, Q., Moore, B., 2004. Satellite-based modeling of gross primary production in an evergreen needleleaf forest. Remote Sens. Environ. 89, 519–534.

Xiao, J.F., Zhuang, Q.L., Baldocchi, D.D., Law, B.E., Richardson, A.D., Chen, J.Q., Oren, R., Starr, G., Noormets, A., Ma, S.Y., Verma, S.B., Wharton, S., Wofsy, S.C., Bolstad, P.V., Burns, S.P., Cook, D.R., Curtis, P.S., Drake, B.G., Falk, M., Fischer, M.L., Foster, D.R., Gu, L.H., Hadley, J.L., Hollinger, D.Y., Katul, G.G., Litvak, M., Martin, T.A., Matamala, R., McNulty, S., Meyers, T.P., Monson, R.K., Munger, J.W., Oechel, W.C.U., Schmid, K.T.P., Scott, H.P., Sun, R.L., Suyker, G., Torn, A.E.M.S., 2008. Estimation of net ecosystem carbon exchange for the conterminous United States by combining MODIS and AmeriFlux data. Agric. For. Meteorol. 148, 1827–1847.

Yu, G., Wen, X., Sun, X., Tanner, B.D., Lee, X., Chen, J., 2006. Overview of ChinaFLUX and evaluation of its eddy covariance measurement. Agric. For. Meteorol. 137, 125–137.

Yuan, W.P., Liu, S., Zhou, G.S., Zhou, G.Y., Tieszen, L.L., Baldocchi, D., Bernhofer, C., Gholz, H., Goldstein, A.H., Goulden, M.L., Hollinger, D.Y., Hu, Y., Law, B.E., Stoy, P.C., Vesala, T., Wofsy, S.C., 2007. Deriving a light use efficiency model from eddy covariance flux data for predicting daily gross primary production across biomes. Agric. For. Meteorol. 143, 189–207.

Yuan, W., Luo, Y., Li, X., Liu, S., Yu, G., Zhou, T., Bahn, M., Black, A., Desai, A.R., Cescatti, A., Marcolla, B., Jacobs, C., Chen, J., Aurela, M., Bernhofer, C., Gielen, B., Bohrer, G., Cook, D.R., Dragoni, D., Dunn, A.L., Gianelle, D., Grünwald, T., Ibrom, A., Leclerc, M.Y., Lindroth, A., Liu, H., Marchesini, L.B., Montagnani, L., Pita, G., Rodeghiero, M., Rodrigues, A., Starr, G., Stoy, P.C., 2011. Redefinition and global estimation of basal ecosystem respiration rate. Glob. Biogeochem. Cycles 25, GB4002, http://dx.doi.org/10.1029/2011GB004150.

Yvon-Durocher, G., Caffrey, J.M., Cescatti, A., Dossena, M., del Giorgio, P., Gasol, J.M., Montoya, J.M., Pumpanen, J., Staehr, P.A., Trimmer, M., Woodward, G., Allen, A.P., 2012. Reconciling the temperature dependence of respiration across timescales and ecosystem types. Nature 487, 472–476.

Zhang, J., Hu, Y., Xiao, X., Chen, P., Han, S., Song, G., Yu, G., 2009. Satellite-based estimation of evapotranspiration of an old-growth temperate mixed forest. Agric. For. Meteorol. 149, 976–984.

Zhou, Z., Jiang, L., Du, E., Hu, H., Li, Y., Chen, D., Fang, J., 2013. Temperature and substrate availability regulate soil respiration in the tropical mountain rainforests, Hainan Island, China. J. Plant Ecol. 6, 325–334.